Generation of correlated and anticorrelated multiple fields via atomic spin coherence

Xihua Yang,[1,2,*] Jiteng Sheng,[1] Utsab Khadka,[1] and Min Xiao[1,†]
[1]*Department of Physics, University of Arkansas, Fayetteville, Arkansas 72701, USA*
[2]*Department of Physics, Shanghai University, Shanghai 200444, People's Republic of China*
(Received 12 July 2011; published 18 January 2012)

We report the experimental observation of generation of four and six strongly correlated and anticorrelated laser fields via atomic spin coherence in triple- and quadruple-Λ-type ^{85}Rb atomic systems. The anticorrelated Stokes and anti-Stokes fields, simultaneously produced through scattering of the applied laser fields off the atomic spin coherence established in advance by the coupling and probe fields, are also highly anticorrelated, respectively, with the corresponding scattering fields. This method can, in principle, be used to create correlated and anticorrelated narrowband multiple fields of any desired order with long correlation times. It paves the way to further study of the generation of multifield quantum correlations and anticorrelations of arbitrarily high order.

DOI: 10.1103/PhysRevA.85.013824 PACS number(s): 42.50.Gy, 32.80.Qk, 42.65.Dr

I. INTRODUCTION

Generation of multiphoton correlations or entanglement is the key requirement for quantum communication and quantum-information processing [1,2]. Previously, the method most commonly used has been to employ linear optical elements, such as mirrors and polarizing beam splitters, to combine photon pairs created through parametric down-conversion processes in nonlinear optical crystals to produce correlated or entangled multiple photons, and up to six correlated or entangled photons have been experimentally realized [3]; however, the generated multiple photons suffer from broad bandwidths and short correlation times (∼picoseconds). By use of nondegenerate four-wave mixing (FWM) or Raman scattering processes in an atomic ensemble, double-Λ-type systems based on electromagnetically induced transparency [4] (EIT) have been actively studied for creating correlated or entangled narrowband photon pairs [5–10], which can benefit from the cancellation of resonant absorption and, at the same time, the resonant enhancement of optical nonlinearity; in addition, the correlation time is determined by the long coherence decay time (∼microseconds) between the two lower states, which is quite suitable for the quantum memory required in a scalable quantum repeater for the realization of long-distance quantum communication [5,7,8]. As a step toward the realization of quantum correlations and anticorrelations or entanglement, intensity correlations or anticorrelations between two or four fields have been studied in atomic ensembles with EIT or FWM methods [11,12]. However, so far no scheme has been proposed to create correlated or anticorrelated multiple fields to any desired order in an atomic ensemble.

In this paper, we report the experimental observation of strong correlations and anticorrelations among four and six laser fields via atomic spin coherence in triple- and quadruple-Λ-type ^{85}Rb atomic systems. The atomic spin coherence created in advance by the coupling and probe fields plays a similar role to the polarizing beam splitter used in the conventional method of generating multiphoton correlations or entanglement through the parametric down-conversion process. This method provides a convenient way to generate correlated and anticorrelated narrowband multiple fields of arbitrarily high order with long correlation times in an atomic ensemble.

II. EXPERIMENT

Figure 1(a) schematically shows the relevant energy levels and the applied and generated laser fields forming a quadruple-Λ-type system. Levels $|1\rangle$, $|2\rangle$, and $|3\rangle$ correspond, respectively, to the ground-state hyperfine levels $5S_{1/2}$ ($F = 2$) and $5S_{1/2}$ ($F = 3$), and the excited state $5P_{1/2}$ in the D_1 line of ^{85}Rb with ground-state hyperfine splitting of 3.036 GHz. The probe field E_p (with frequency ω_p and Rabi frequency Ω_p) and coupling field E_c (with frequency ω_c and Rabi frequency Ω_c) are tuned to resonance with the transitions $|1\rangle$-$|3\rangle$ and $|2\rangle$-$|3\rangle$, respectively. A third mixing field E_m, which is generated from the coupling field with an 812 MHz acousto-optic modulator (AOM), off-resonantly couples levels $|2\rangle$ and $|3\rangle$. As analyzed in Ref. [13], a Stokes field E_s (with frequency ω_s and Rabi frequency Ω_s) and an anti-Stokes field E_{ap} (with frequency ω_{ap} and Rabi frequency Ω_{ap}) can be simultaneously created through FWM processes with both the coupling and probe fields acting on both $|1\rangle$-$|3\rangle$ and $|2\rangle$-$|3\rangle$ transitions at high atomic density as well as high coupling and probe powers, where two coupling (probe) photons are converted into one Stokes (anti-Stokes) photon and one probe (coupling) photon. Moreover, another anti-Stokes field E_{am} can also be produced through the FWM process, involving the coupling, probe, and mixing fields, where one probe photon and one mixing photon are converted into one coupling photon and one anti-Stokes photon. In fact, these three simultaneously generated FWM fields can be equivalently viewed as scattering the coupling, probe, and mixing fields off the atomic spin coherence (ρ_{12}) established in advance by the coupling and probe fields in the Λ-type EIT configuration formed by levels $|1\rangle$, $|2\rangle$, and $|3\rangle$ [14]. The equivalent configuration is shown in Fig. 1(b), which can be readily extended to an N-Λ-type (N is a positive integer) system by applying more laser fields tuned to the vicinity of the transitions $|1\rangle$-$|3\rangle$ and/or $|2\rangle$-$|3\rangle$ to mix with the atomic spin coherence.

The experimental setup is similar to our previous one used to generate two controllable FWM fields [15]. The three

*yangxih@yahoo.com.cn
†mxiao@uark.edu

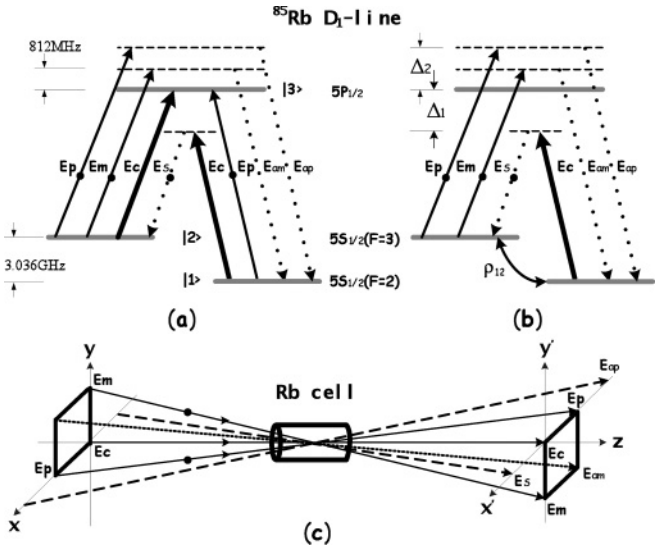

FIG. 1. (a) The quadruple-Λ-type system of the D_1 transitions of the ^{85}Rb atom coupled by the coupling E_c, probe E_p, and mixing E_m fields, and the corresponding generated Stokes E_s and anti-Stokes E_{ap} and E_{am} fields. (b) The equivalent configuration to (a) with the two lower states driven by the induced coherent spin wave ρ_{12} created in advance by the E_c and E_p fields in the Λ-type EIT configuration. (c) The geometry used in the experiment.

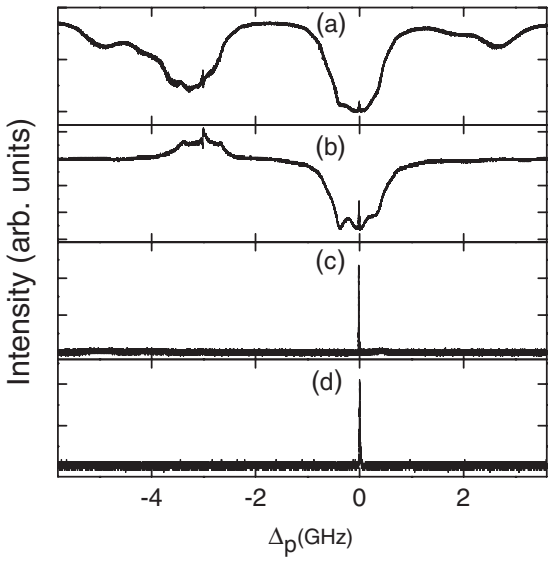

FIG. 2. (a) The transmission spectrum of the probe field of the D_1 lines of ^{85}Rb and ^{87}Rb as a function of the probe detuning Δ_p from the $5S_{1/2}(F = 2)$-$5P_{1/2}(F = 3)$ transition, with the coupling field tuned to resonance with the $5S_{1/2}(F = 3)$-$5P_{1/2}(F = 3)$ transition under $E_p = 10$ mW, $E_c = 12$ mW, and $T = 100\,^{\circ}$C. (b),(c),(d) The corresponding transmitted coupling field intensity and the generated anti-Stokes E_{ap} and Stokes E_s signals.

input laser beams are carefully aligned spatially on the three corners of a square-box pattern as indicated in Fig. 1(c). The horizontally polarized coupling laser beam (with a waist radius of about 450 μm and wavelength of about 794.98 nm) is produced from a cw Ti:sapphire laser; the vertically polarized probe beam (with wavelength of about 795 nm and a waist similar to that of the coupling beam) is from an external-cavity diode laser; and the mixing laser beam (with a waist of about 240 μm and a vertical polarization) is produced from the split beam of the cw Ti:sapphire laser by using an AOM. After combination on a polarizing beam splitter, the three laser beams with their respective waists nearly at the center of a 7.6-cm-long Rb vapor cell are aligned to maintain good spatial overlap, and they propagate through the atomic medium in the same direction with small angles (about 0.3°) between them. This arrangement satisfies the two-photon Doppler-free condition for Λ-type subsystems [16]. According to the phase-matching condition, the generated Stokes field E_s with vertical polarization and anti-Stokes field E_{ap} with horizontal polarization propagate in the directions of E_s and E_{ap}, that is, at the same coupling-probe angle but on the opposite sides of the coupling and probe beams, and the generated anti-Stokes field E_{am} with horizontal polarization is in the direction of E_{am}, i.e., at the lower right corner of the right-hand square box, respectively, as shown in Fig. 1(c). These three signals are detected by three avalanche photodiode detectors, and the transmitted coupling, probe, and mixing beams are simultaneously monitored by three photodiodes. The Rb vapor cell consisting of both ^{85}Rb and ^{87}Rb isotopes with 3 Torr Ne buffer gas is wrapped in μ metal for magnetic shielding, and typically operated at a temperature of about $T = 100\,^{\circ}$C (corresponding to an atomic density of about 6×10^{12} cm^{-3}).

III. RESULTS AND DISCUSSION

We first investigate the generation of four-field correlations and anticorrelations via atomic spin coherence in a triple-Λ-type system by blocking the mixing field. Figures 2(a) and 2(b) show the transmitted intensities of the probe and coupling fields as functions of the probe detuning $\Delta_p = \omega_p - \omega_{31}$ from the $5S_{1/2}(F = 2)$-$5P_{1/2}(F = 3)$ transition, with the coupling field tuned to resonance with the $5S_{1/2}(F = 3)$-$5P_{1/2}(F = 3)$ transition under optical powers of about $E_p = 10$ mW and $E_c = 12$ mW (corresponding to Rabi frequencies Ω_p and Ω_c of about 40 MHz), respectively. The frequency of the coupling field is identified from the saturated absorption spectrum by using another reference Rb cell. As seen in Figs. 2(a) and 2(b), when the probe field is tuned to resonance with the transition $5S_{1/2}(F = 2)$-$5P_{1/2}(F = 3)$, a narrow EIT window is observed in the probe field transmission spectrum due to the two-photon Doppler-free configuration used in the Doppler-broadened atomic medium [16], and the transmitted coupling field also exhibits a narrow EIT window due to coherent population trapping [4]. The corresponding generated anti-Stokes E_{ap} and Stokes E_s fields are shown in Figs. 2(c) and 2(d), respectively.

Figure 3(A) depicts the typical time traces of the intensity fluctuations of the anti-Stokes E_{ap}, Stokes E_s, coupling E_c, and probe E_p fields with the coupling and probe fields tuned to resonance with the transitions $5S_{1/2}(F = 3)$-$5P_{1/2}(F = 3)$ and $5S_{1/2}(F = 2)$-$5P_{1/2}(F = 3)$, respectively; the presented data are parts of the 5 ms recorded traces. It is evident that the four fields fluctuate in a highly correlated or anticorrelated manner at EIT resonance, although independent coupling and probe fields are employed. The strongly anticorrelated Stokes and anti-Stokes fields are also

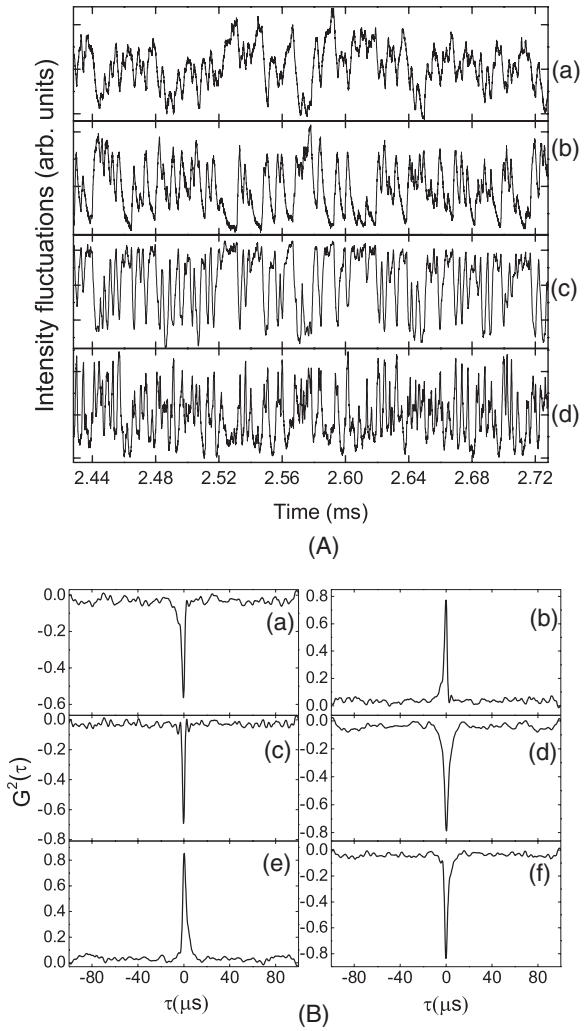

FIG. 3. (A) The time traces of the intensity fluctuations of the anti-Stokes E_{ap} (a), Stokes E_s (b), coupling (c), and probe (d) fields with the coupling and probe fields tuned to resonance with the transitions $5S_{1/2}(F = 3)$-$5P_{1/2}(F = 3)$ and $5S_{1/2}(F = 2)$-$5P_{1/2}(F = 3)$, respectively; the presented data are parts of the 5 ms recorded traces. (B) The time-delay intensity correlation functions of $G^{(2)}_{p-ap}(\tau)$ (a), $G^{(2)}_{p-s}(\tau)$ (b), $G^{(2)}_{p-c}(\tau)$ (c), $G^{(2)}_{ap-s}(\tau)$ (d), $G^{(2)}_{ap-c}(\tau)$ (e), and $G^{(2)}_{s-c}(\tau)$ (f).

anticorrelated with the coupling and probe fields, respectively. The time-delay intensity correlation function $G^{(2)}_{ij}(\tau)$ between the two laser fields i and j is given by $G^{(2)}_{ij}(\tau) = \langle \delta I_i(t)\delta I_j(t+\tau)\rangle / \sqrt{\langle [\delta I_i(t)]^2\rangle \langle [\delta I_j(t+\tau)]^2\rangle}$ [12], where $\delta I_{i,j}(t) = I_{i,j}(t) - \langle I_{i,j}(t)\rangle$ are the time-dependent intensity fluctuations with $\langle I_{i,j}\rangle$ being the average intensities of the laser fields and $i, j = c, p, s, ap$ the labels to designate the coupling, probe, Stokes E_s, and anti-Stokes E_{ap} fields, respectively. The intensity correlation functions $G^{(2)}_{ij}(\tau)$ between different pairs of the four fields are displayed in Fig. 3(B). These correlation functions have sharp peaks and dips at time delay nearly equal to zero with corresponding amplitudes of about −5.7, 0.78, −0.69, −0.80, 0.86, and −0.83, respectively, implying strong temporal positive and negative correlations in the intensity fluctuations of the four fields; and the correlation times (of approximately 3–5 μs) correspond to the decay time of the atomic spin coherence, which is far longer than that of the photon pairs produced through parametric down-conversion in nonlinear optical crystals [3]. The small time delay (of about 50–350 ns) in the arrival time between different pairs of the four fields results from the combination of FWM processes in the triple-Λ system and field propagation through the vapor cell [7,10].

The highly correlated and anticorrelated features among the four fields can be well understood in terms of the interaction between the laser fields and the atomic medium. As shown in Fig. 1(a), the Stokes E_s and anti-Stokes E_{ap} fields are generated through two FWM processes, where every Stokes (anti-Stokes) photon generation is accompanied by the depletion of two coupling (probe) photons and the generation of one probe (coupling) photon. FWM is a parametric process, which leads to the generation of Stokes (anti-Stokes) and probe (coupling) photons in pairs and to subsequent intensity correlations between them [10]. However, the two FWM processes for producing the Stokes and anti-Stokes fields share the same coupling and probe fields and compete with each other, which leads to the strong anticorrelations between the Stokes and anti-Stokes fields, as well as between the coupling and probe fields.

Physical insight into the correlations and anticorrelations among the four fields can be obtained by solution of the density-matrix equations together with the field propagation equations. The anti-Stokes and Stokes fields can be readily treated as generated through scattering of the probe and coupling fields off the atomic spin coherence [14,15]. In the middle Λ-type subsystem, when the coupling and probe fields are resonant with the respective transitions, ignoring the depletion of the atomic spin coherence, the corresponding density-matrix elements are

$$\rho_{11}^{(0)} = \frac{\Omega_c^2}{\Omega_c^2 + \Omega_p^2}, \quad \rho_{22}^{(0)} = \frac{\Omega_p^2}{\Omega_c^2 + \Omega_p^2}, \quad \rho_{12}^{(0)} = \frac{-\Omega_p \Omega_c^*}{\Omega_c^2 + \Omega_p^2}$$

[14], which can be regarded as the initial conditions of the density-matrix equations for the Raman scattering processes that generate the anti-Stokes and Stokes fields. As the Rabi frequencies (about tens of megahertz) of the scattering fields are far smaller than their detunings (about 3 GHz), the coupling between the scattering fields can be neglected, and we can obtain an approximate solution of the density-matrix equations to first order in the scattering fields. Thus, for the case of the anti-Stokes Raman scattering process, the atomic polarizations ρ_{31} and ρ_{32} at steady state can be written as

$$\rho_{31} = \frac{j\Omega_{ap}\left(\rho_{11}^{(0)} - \rho_{33}^{(0)}\right) + j\Omega_p \rho_{21}^{(0)}}{\gamma_{31} - j\Delta_2}, \tag{1}$$

$$\rho_{32} = \frac{j\Omega_{p}\left(\rho_{22}^{(0)} - \rho_{33}^{(0)}\right) + j\Omega_{ap} \rho_{12}^{(0)}}{\gamma_{32} - j\Delta_2}, \tag{2}$$

where the detuning of the probe (anti-Stokes) field from the resonant transition $|2\rangle$-$|3\rangle$ ($|1\rangle$-$|3\rangle$) is $\Delta_2 = \omega_p - \omega_{32} = \omega_{ap} - \omega_{31}$, and γ_{31} (γ_{32}) is the coherence decay rate between states $|1\rangle$ ($|2\rangle$) and $|3\rangle$. Similar expressions for the atomic polarizations ρ_{31} and ρ_{32} for the Stokes Raman scattering process can be obtained by replacing Δ_2, Ω_{ap}, and Ω_p with Δ_1 ($= \omega_c - \omega_{31} = \omega_s - \omega_{32}$), Ω_c, and Ω_s, respectively.

In the present triple-Λ-type system, the stimulated Raman scattering processes for generating Stokes and anti-Stokes fields become dominant at high atomic density as well as high coupling and probe field powers, and, in fact, can be regarded as two FWM processes. Thus, the intensity fluctuations of the four fields mainly result from the nonlinear FWM processes [12]. Assuming that at an arbitrary time there is a fluctuation in the absorption of either the probe or coupling field, the populations of the two lower states will fluctuate accordingly. Under EIT conditions, because $\rho_{33}^{(0)} = 0$ and $\dot{\rho}_{11}^{(0)} + \dot{\rho}_{22}^{(0)} = 0$, it is possible to assume $\rho_{11}^{(0)} = \frac{\Omega_c^2}{\Omega_c^2+\Omega_p^2} + f(t)$ and $\rho_{22}^{(0)} = \frac{\Omega_p^2}{\Omega_c^2+\Omega_p^2} - f(t)$, where $f(t)$ is the population fluctuation with a real value. As analyzed in Ref. [12], the intensity fluctuations of the probe (Stokes) and coupling (anti-Stokes) fields are proportional to the imaginary parts of the fluctuations of the corresponding atomic polarizations (i.e., $\mathrm{Im}\delta\rho_{32}$ and $\mathrm{Im}\delta\rho_{31}$), respectively. Obviously, it can be seen from Eqs. (1) and (2) that a decrease in the probe (or coupling) field's intensity will result in an increase in the anti-Stokes (or Stokes) field's intensity. Moreover, absorption of the coupling (or probe) field is always accompanied by the amplification of the probe (or coupling) field. As a consequence, the intensity fluctuations among the four fields exhibit strong correlations and anticorrelations.

The above scheme can be generalized to include more laser fields, tuned to the vicinity of the transitions $|1\rangle$-$|3\rangle$ and/or $|2\rangle$-$|3\rangle$, for generating more correlated and anticorrelated fields, basically to any desired order. When the detunings of the scattering fields are sufficiently large compared to their Rabi frequencies, different pairs of the scattering fields and the corresponding generated fields can be treated separately. In this case, according to the above analysis, the correlated up-converted frequency components (i.e., anti-Stokes fields) are anticorrelated with the down-converted frequency components (i.e., Stokes fields), all of which are anticorrelated with the corresponding scattering fields as well. These correlated relations are confirmed by our experimental observation of six-field correlations and anticorrelations when an additional mixing field E_m is applied. Figure 4(A) gives the time traces of the intensity fluctuations of the applied probe, coupling, and mixing fields, as well as the generated Stokes E_s, anti-Stokes E_{ap}, and E_{am} fields under the conditions $E_p =$ 10 mW, $E_c = 12$ mW, and $E_m = 0.45$ mW with the coupling and probe fields tuned to resonance with the transitions $5S_{1/2}(F = 3)$-$5P_{1/2}(F = 3)$ and $5S_{1/2}(F = 2)$-$5P_{1/2}(F = 3)$, respectively. As seen in Fig. 4(A), the intensity fluctuations of the six fields exhibit strong correlations and anticorrelations. The anticorrelated Stokes field E_s and anti-Stokes field E_{ap} (or E_{am}) are also strongly anticorrelated, respectively, with the coupling and probe (or mixing) fields. There are 15 corresponding time-delay intensity correlation functions with similar features to those shown in Fig. 3(B). Figure 4(B) displays the peak amplitudes of the 15 intensity correlation functions for various pairs of the six fields. It is obvious that strong correlations and anticorrelations in the intensity fluctuations exist among these six fields.

It is worth noting that the present EIT-based multiple-Λ-type configurations have several notable features. First, compared to the commonly used scheme for producing correlated or entangled multiphotons through the parametric down-conversion process by using polarizing beam splitters [3], the current scheme can generate any desired number of correlated and anticorrelated narrowband fields with long correlation times. Since the correlation time is determined by the decay time of the spin coherence, it can be long in practice (e.g., of the order of milliseconds or seconds for cold atomic ensembles), which would be very useful for quantum memory [5,7,8]. Second, in this EIT-based scheme, the created atomic spin coherence plays a role analogous to that of the polarizing beam splitter used in the conventional way to generate multiple correlated photons through

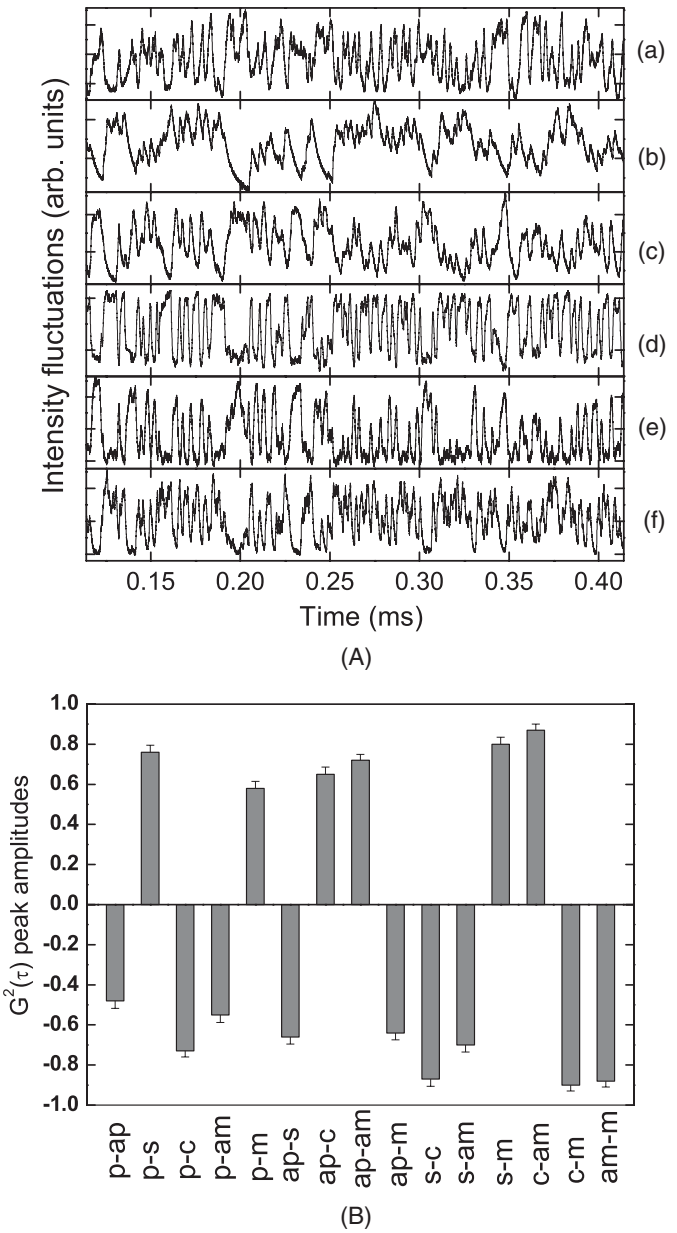

FIG. 4. (A) The time traces of the intensity fluctuations of the probe (a), anti-Stokes E_{ap} (b), Stokes E_s (c), coupling (d), mixing (e), and anti-Stokes E_{am} (f) fields, with the coupling and probe fields tuned to resonance with the transitions $5S_{1/2}(F = 3)$-$5P_{1/2}(F = 3)$ and $5S_{1/2}(F = 2)$-$5P_{1/2}(F = 3)$, respectively. (B) The peak amplitudes (with error bars) of the corresponding 15 time-delay intensity correlation functions between different pairs of the six fields.

parametric down-conversion; however, there is a critical difference between them, i.e., the atomic medium acts as a nonlinear element for the FWM, whereas the polarizing beam splitter is a linear element. Third, the anticorrelation in the present scheme enables the manipulation of the relative intensities of the generated Stokes and anti-Stokes E_{ap} (or E_{am}) fields by variation of the coupling field intensity [15], which differs from photon-pair generation through Raman scattering [5–9] or EIT [10] in a double-Λ system, where the produced photon pairs are always correlated and their intensities increase or decrease synchronously. Finally, compared to the generation of four-field correlations and anticorrelations, the experimental realization of six correlated and anticorrelated fields simultaneously is a significant advance in the field. In fact, it has given a clear demonstration that this scheme can be extended to generate multiple correlated and anticorrelated fields to arbitrarily high order via atomic spin coherence.

IV. SUMMARY

In conclusion, we have experimentally demonstrated the generation of four and six highly correlated and anticorrelated laser fields via atomic spin coherence formed via the EIT configuration with independent coupling and probe fields in triple- and quadruple-Λ-type ^{85}Rb atomic systems. This method provides a proof-of-principle demonstration of a convenient way to generate correlated and anticorrelated narrowband multiple fields of any desired order with long correlation times in an atomic ensemble. Further work will be performed to study the quantum nature of the correlation properties among these fields in a similar way to that utilized in Ref. [10], by observing the violation of a Cauchy-Schwarz inequality, and to find possible applications in quantum communication and quantum-information processing.

ACKNOWLEDGMENTS

This work is supported in part by the National Science Foundation of the US. X.Y. is supported by the National Natural Science Foundation of China (Grants No. 10974132 and No. 50932003), the Innovation Program of Shanghai Municipal Education Commission (Grant No. 10YZ10), the China Scholarship Council (Grant No. 2009831291), and the Shanghai Leading Academic Discipline Project (Grant No. S30105).

[1] D. Bouweester, A. Ekert, and A. Zeilinger, *The Physics of Quantum Information* (Springer-Verlag, Berlin, 2000).

[2] M. A. Nielsen and I. L. Chuang, *Quantum Computation and Quantum Information* (Cambridge University Press, Cambridge, 2000).

[3] P. G. Kwiat *et al.*, Phys. Rev. Lett. **75**, 4337 (1995); C. Y. Lu *et al.*, Nat. Phys. **3**, 91 (2007).

[4] S. E. Harris, Phys. Today **50**(9), 36 (1997); M. Xiao *et al.*, Phys. Rev. Lett. **74**, 666 (1995); M. Fleischhauer, A. Imamoglu, and J. P. Marangos, Rev. Mod. Phys. **77**, 633 (2005).

[5] L. M. Duan, M. D. Lukin, J. I. Cirac, and P. Zoller, Nature (London) **414**, 413 (2001).

[6] M. D. Lukin *et al.*, Phys. Rev. Lett. **82**, 1847 (1999); M. D. Lukin, P. R. Hemmer, and M. O. Scully, Adv. At. Mol. Opt. Phys. **42**, 347 (2000).

[7] C. H. van der Wal *et al.*, Science **301**, 196 (2003); A. Kuzmich *et al.*, Nature (London) **423**, 731 (2003).

[8] N. Sangouard, C. Simon, H. de Riedmatten, and N. Gisin, Rev. Mod. Phys. **83**, 33 (2011).

[9] V. Balic *et al.*, Phys. Rev. Lett. **94**, 183601 (2005); H. Wu and M. Xiao, Phys. Rev. A **80**, 063415 (2009).

[10] A. M. Marino, V. Boyer, and P. D. Lett, Phys. Rev. Lett. **100**, 233601 (2008); V. Boyer *et al.*, Science **321**, 544 (2008).

[11] C. L. Garrido-Alzar *et al.*, Europhys. Lett. **61**, 485 (2003); K. Motomura, M. Tsukamoto, A. Wakiyama, K. Harada, and M. Mitsunaga, Phys. Rev. A **71**, 043817 (2005); K. Harada, H. Hayashi, K. Mori, and M. Mitsunaga, J. Opt. Soc. Am. B **25**, 40 (2008).

[12] V. A. Sautenkov, Y. V. Rostovtsev, and M. O. Scully, Phys. Rev. A **72**, 065801 (2005); G. O. Ariunbold *et al.*, J. Mod. Opt. **57**, 1417 (2010); L. S. Cruz *et al.*, Eur. Phys. J. D **41**, 531 (2006).

[13] K. I. Harada *et al.*, Phys. Rev. A **73**, 013807 (2006); G. S. Agarwal, T. N. Dey, and D. J. Gauthier, *ibid.* **74**, 043805 (2006); K. I. Harada *et al.*, *ibid.* **78**, 013809 (2008).

[14] A. J. Merriam *et al.*, Phys. Rev. Lett. **84**, 5308 (2000).

[15] X. H. Yang, J. T. Sheng, U. Khadka, and M. Xiao, Phys. Rev. A **83**, 063812 (2011).

[16] J. Gea-Banacloche, Y. Li, S. Jin, and M. Xiao, Phys. Rev. A **51**, 576 (1995).